

# Analysis and control of nonlinear vibration of autonomous vehicle passing through hybrid consecutive speed control humps

Zhiyong YANG<sup>1,2</sup> , Long WANG<sup>2</sup>, Yanjun YU<sup>2</sup>, Zhenping MOU<sup>2</sup>, and Minghui OU<sup>1,2</sup>

<sup>1</sup>Chongqing Vocational Institute of Engineering, Chongqing 402260, PR China

<sup>2</sup>College of Computer and Information Science, Chongqing Normal University, Chongqing 401331, PR China

**Abstract.** In order to improve the safety and comfort of autonomous vehicles passing through the expressway, relevant departments of expressway construction often design and lay consecutive speed control humps (SCHs) with cross-sections of different shapes according to different road conditions, such as the combination of trapezoidal and sinusoidal SCHs. In this paper, we conduct a study about the nonlinear dynamic characteristics of the autonomous vehicle passing through hybrid SCHs. Firstly, a four-degree-of-freedom (4-DOF) nonlinear model of the vehicle suspension and the speed coupling excitation model under hybrid SCHs are established. Then the fourth-fifth order Runge–Kutta method is used to simulate the nonlinear system, and its nonlinear dynamic characteristics are analyzed. The results show that chaotic motion occurs when the vehicle passes through hybrid SCHs, and the speed range of chaotic motion is obtained. Then, a direct variable feedback control method is used to suppress the chaotic vibration of semi-active suspension vehicles, and the effect is verified by simulation experiments. Finally, this paper presents a multi-objective optimization model based on a genetic algorithm (GA) for active suspension vehicles. The optimization model selects the vertical displacement and pitching angle of the vehicle body as the objective function. The research results of this paper can provide information on the ride comfort's optimization for autonomous vehicles passing through hybrid SCHs and on the design of vehicle suspension system.

**Key words:** autonomous vehicle; hybrid consecutive speed control humps; nonlinear vibration; safety and comfort.

## 1. INTRODUCTION

Automatic driving is one of the main directions of intelligent and networked development in the field of automobile industry and transportation. With the rapid development of artificial intelligence, the internet of things and other related technologies, automatic driving technology is also constantly improving and become ever more innovative. For vehicles, safety and comfort are important factors affecting passengers' choice, and they are also the hot point issues of current research [1, 2]. The vehicle suspension system plays a significant part in improving vehicle driving safety and comfort [3]. It contains many nonlinear elements, which also leads to complex dynamic characteristics, including bifurcation and chaos [4, 5]. Chaotic motion will not only affect the comfort of the vehicle, but may also damage the road surface and have an impact on safety [6]. The current research has noticed that the vehicle suspension system is one of the factors that have an important impact on the vehicle amplitude and vibration intensity [5, 7, 8]. Under extreme conditions, severe vibration may damage the suspension system and even cause traffic accidents [9, 10].

As for the selection of the vehicle simulation model, the four-degree-of-freedom (4-DOF) half-vehicle model is closer to the

practical vehicle model [9]. The model can not only reflect the vertical and pitching motion of a vehicle body, but also the vertical direction deformation when the front and rear wheels move [11].

Combinations of speed control humps (SCHs) with cross-sections of different shapes have begun to appear on highways. This type of SCHs is referred to as hybrid SCHs in this paper. The difference between hybrid SCHs and ordinary SCHs is that the cross-section of ordinary SCHs is stable, such as e.g. a trapezoid, while the cross-section of hybrid SCHs is a combination of different shapes, such as a trapezoid and sinusoid. Ordinary SCHs have proved to have a certain impact on the comfort of the vehicle [11, 12], while research on hybrid SCHs is relatively lacking: whether the chaotic motion will occur, what range the speed should be controlled in in order to improve comfort and safety, and how to effectively suppress chaotic motion if there is chaotic motion. As a potential scene in the automatic driving scene, it is of practical significance to research the nonlinear motion characteristics of vehicles passing through hybrid SCHs. Taking the combination of trapezoidal and sinusoidal SCHs as an example, this paper establishes the speed coupling excitation model. Through MATLAB simulation, the nonlinear motion characteristics of the 4-DOF vehicle model excited by this hybrid SCHs are analyzed experimentally, and the law of chaotic motion is obtained.

Nowadays, on the basis of the different control force, the vehicle suspension is divided into three types: passive, semi-

\*e-mail: zyy@cqvie.edu.cn

Manuscript submitted 2022-05-15, revised 2022-09-01, initially accepted for publication 2022-09-25, published in December 2022.

active and active. Although passive suspension has a low cost, it is difficult to adapt it to complex road conditions. The semi-active suspension with controllable stiffness or damping has the advantages of simple structure, stability and low cost [13]. The design of a direct variable feedback control method of the semi-active suspension is simple and practical, which is proposed and used in this paper. The simulation results show that when the vehicle passes through hybrid SCHs, it can effectively suppress the chaotic motion, improving the safety and comfort of passengers.

Active suspension with controllable power is praised for its excellent damping performance and its active control force can be adjusted. Genetic algorithm (GA) is a search algorithm used to solve optimization problems [14]. It is a type of evolutionary algorithm based on the idea of natural selection and genetics. It has been used widely in seeking the optimal parameters of vehicle suspension design [15–18]. In this paper, a multi-objective optimization model based on GA with elite strategy is proposed to seek the optimal speed and active control force of active suspension vehicles, so as to improve driving comfort and safety when passing through hybrid SCHs.

The second part of this paper introduces the speed coupling excitation model in the case of the SCHs with the combination of the trapezoidal and the sinusoidal section. The 4-DOF nonlinear suspension vehicle model and relevant simulation parameters are described, too. In the third part, we use MATLAB to conduct the simulation experiment. The nonlinear dynamic characteristics of vehicles passing through hybrid SCHs are analyzed by means of the nonlinear feature extraction methods such as the bifurcation diagram and Poincaré map. In the fourth part, the direct variable negative feedback regulation method is proposed, and the effect of chaotic vibration control is verified by experiments. In the fifth part, the paper introduces the multi-objective optimization model based on GA, while experiments and analysis are conducted. The sixth part summarizes the paper.

## 2. SIMULATION MODEL DESCRIPTION

### 2.1. SCHs excitation model

We use the wave in Fig. 1 to approximately simulate the excitation of the combination of trapezoidal and sinusoidal SCHs, where  $h$  and  $p$  is the height and width of trapezoidal SCHs, respectively. Meanwhile,  $u$  and  $q$  is the height and width of sinusoidal SCHs, respectively.  $d$  is the distance between two adjacent speed-control bumps. To guarantee stability, safety and effective deceleration when a vehicle passes consecutive SCHs, the average of  $h$  and  $u$ , are set to 1.0 cm–3.0 cm,  $p$  and  $q$  are 50 cm–100 cm,  $d$  is 50 cm–100 cm empirically.  $t_p = p/v$  are

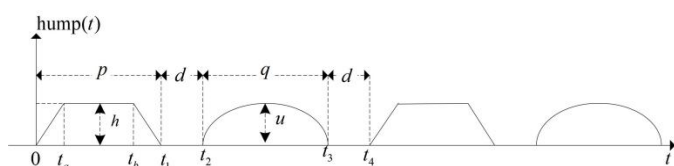


Fig. 1. Consecutive SCH's geometric shape

respectively the time to pass the trapezoidal SCHs, the sinusoidal SCHs and the gap between two adjacent humps. Therefore, we use  $T = t_p + t_d + t_q + t_d$  to indicate the incentive period, and the relationship between excitation frequency  $f$  and vehicle speed  $v$  can be calculated as:

$$f = \frac{1}{T} = \frac{v}{p + q + 2d}. \quad (1)$$

Considering the influence of pavement roughness, the incentive of front wheel can be represented as:

$$x_{fd} = \text{hump}(t) + A \cdot \sin(2\pi f_1 t). \quad (2)$$

In our paper,  $A$  is the approximate road surface roughness amplitude,  $f_1$  is the intrinsic excitation frequency owing to road surface roughness, and  $\text{hump}(t)$  can be expressed as follows:

$$\text{hump}(t) = \begin{cases} \frac{h}{t_a} \cdot t, & 0 < t \leq t_a, \\ h, & t_a < t \leq t_b, \\ \frac{h}{t_1 - t_b} \cdot (t_1 - t), & t_b < t \leq t_1, \\ 0, & t_1 < t \leq t_2, \\ u \cdot \sin\left(\frac{\pi}{t_q} \cdot \left(t - \frac{T}{2}\right)\right), & t_2 < t \leq t_3, \\ 0, & t_3 < t \leq t_4. \end{cases} \quad (3)$$

The lag between the front and rear wheels can be understood as the time difference between the two wheels when the front wheel passes a point on the road and the rear wheel passes that point at the same speed, which is calculated as:

$$\Delta t = \frac{l_f + l_r}{v}, \quad (4)$$

where  $l_f$  and  $l_r$  are the distances between the front and rear wheel and the center of the vehicle.

Thus, rear wheel excitation can be defined as:

$$x_{rd} = \text{hump}(t + \Delta t). \quad (5)$$

From equation (1) and equation (4),  $\Delta t$  can be also expressed as:

$$\Delta t = \frac{T(l_f + l_r)}{p + q + 2d}. \quad (6)$$

### 2.2. Nonlinear 4-DOF half-vehicle model

The simplified 4-DOF half-vehicle model can be regarded as a completely symmetrical structure, and the vertical displacement, pitching motion of the body as well as deformation of the front and rear wheels need to be considered. The nonlinearity of front and rear suspension springs, front and rear wheels, and suspension dampers are considered, too. The longitudinal view in Fig. 2 is the simplified model of the 4-DOF half-vehicle [5,9]. And the main components of active suspension model are the tire, spring, suspension and unsprung mass.

Table 1 below shows the symbol description of the model.

Analysis and control of nonlinear vibration of autonomous vehicle passing through hybrid consecutive speed control humps

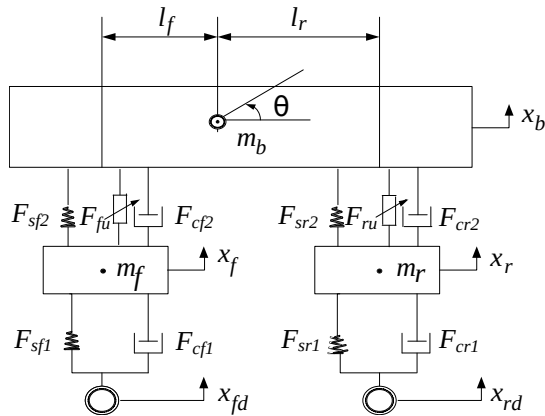


Fig. 2. 4-DOF half-vehicle model

Table 1

Symbol description for the model

Symbol	Symbol description
$m_b$	sprung mass
$\theta$	the angular displacement of $m_b$
$m_f$	front unsprung masses
$m_r$	rear unsprung masses
$l_f$	front lengths
$l_r$	rear lengths
$x_{fd}$	excitations to the front tire
$x_{rd}$	excitations to the rear tire
$x_b$	displacements of $m_b$
$x_f$	displacements of $m_f$
$x_r$	displacements of $m_r$
$F_{sf1}$	front nonlinear suspension damper forces
$F_{sr1}$	rear nonlinear suspension damper forces
$F_{sf2}$	front nonlinear suspension spring forces
$F_{sr2}$	rear nonlinear suspension spring forces
$F_{cf2}$	front suspension damper forces
$F_{cr2}$	rear suspension damper forces
$F_{cf1}$	front nonlinear tire spring forces
$F_{cr1}$	rear nonlinear tire spring forces
$F_{fu}$	active control forces of rear suspensions
$F_{ru}$	active control forces of front suspensions
$J$	the moment of inertia of the pitch axis

Based on the second Newton law, the equations of motion can be made as follows:

$$\begin{cases} m_b \ddot{x}_b = -F_{sf2} - F_{cf2} - F_{sr2} - F_{cr2} + F_{fu} + F_{ru} - m_b g, \\ J \ddot{\theta} = (F_{sf2} + F_{cf2} + F_{fu}) l_f \cos \theta - (F_{sr2} + F_{cr2} + F_{ru}) l_r \cos \theta, \\ m_f \ddot{x}_f = F_{sf2} + F_{cf2} + F_{fu} - F_{sf1} - F_{cf1} - m_f g, \\ m_r \ddot{x}_r = F_{sr2} + F_{cr2} + F_{ru} - F_{cr1} - m_r g. \end{cases} \quad (7)$$

Setting  $x_1 = x_b$ ,  $x_2 = \dot{x}_b$ ,  $x_3 = \theta$ ,  $x_4 = \dot{\theta}$ ,  $x_5 = x_b$ ,  $x_6 = x_f$ ,  $x_7 = x_r$ ,  $x_8 = \dot{x}_r$ , the system state equations can be expressed by:

$$\begin{cases} \dot{x}_1 = x_2, \\ \dot{x}_2 = -\frac{1}{m_b} (F_{sf2} + F_{cf2} + F_{sr2} + F_{cr2} - F_{fu} - F_{ru}) - g, \\ \dot{x}_3 = x_4, \\ \dot{x}_4 = \frac{\cos \theta}{J} [(F_{sf2} + F_{cf2} + F_{fu}) l_f - (F_{sr2} + F_{cr2} + F_{ru}) l_r] - g, \\ \dot{x}_5 = x_6, \\ \dot{x}_6 = -\frac{1}{m_f} (F_{sf2} v + v F_{cf2} v + v F_{fu} v - v F_{sf1} v + v F_{cf1}) - g, \\ \dot{x}_7 = x_8, \\ \dot{x}_8 = -\frac{1}{m_r} (F_{sr2} v + v F_{cr2} v + v F_{ru} v - v F_{sr1} v + v F_{cr1}) - g. \end{cases} \quad (8)$$

### 2.3. Simulation parameters

Figure 2 shows our simulation object, and Table 2 shows the parameters of the model [11]. We set the static equilibrium parameters as the initial conditions of the simulation, and set the step size to 0.02 km/h. We use the fourth-fifth order Runge–Kutta method to solve the differential equation numerically. It uses the fourth-order method to provide candidate solutions, and the fifth-order method to control the error.

Table 2

Specific parameters setting in numerical simulation

Parameter	Value	Parameter	Value
$m_b$	1180.0 kg	$J$	633.615 kg·m <sup>2</sup>
$c_{r1}$	10 kg/s	$m_f$	50.0 kg
$l_f$	1.123 m	$c_{f2u}$	500 kg/s
$m_r$	45.0 kg	$l_r$	1.377 m
$c_{f2d}$	359.7 kg/s	$k_{f1}$	140000.0 N/m
$n_{f1}$	1.25	$c_{r2u}$	500 kg/s
$k_{r1}$	140000.0 N/m	$n_{r1}$	1.25
$c_{r2d}$	359.7 kg/s	$k_{f2}$	36952.0 N/m
$n_{f2}$	1.5	$h$	0.025 m
$k_{r2}$	30130.0 N/m	$n_{r2}$	1.5
$s_1$	500 mm	$g$	9.81 N/kg
$c_{f1}$	10 kg/s	$s_2$	500 mm

## 3. ANALYSIS OF NONLINEAR DYNAMIC CHARACTERISTICS OF AUTONOMOUS VEHICLE PASSING THROUGH THE COMBINATION OF TRAPEZOIDAL AND SINUSOIDAL SCHS

### 3.1. Regional division of velocity bifurcation diagram

The dynamic response of the 4-DOF nonlinear vehicle suspension model under hybrid SCHs excitation is studied by means of the fourth-fifth Runge–Kutta algorithm in MATLAB [19]. The

simulation step is 0.02 km/h, and the vertical displacement's velocity bifurcation diagram of the vehicle body in this paper is shown in Fig. 3.

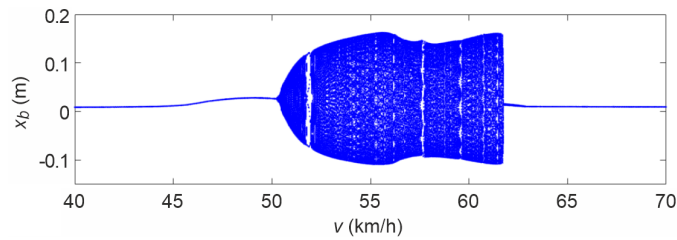


**Fig. 3.** Vertical displacement's velocity bifurcation diagram of the vehicle body

From Fig. 3, the vibration changes significantly and becomes complex with speed varying from 50.50 km/h to 60.60 km/h, which indicates that chaotic responses may occur when the speed is in or close to this unstable range. Therefore, according to the differences in nonlinear characteristics of different velocity segments [4, 9], the whole velocity segment is divided into three areas: A (40.00–50.50 km/h), B (50.50–62.60 km/h), C (62.60–70.00 km/h).

### 3.2. Analysis of dynamic characteristics of each velocity region

In order to further reveal the potential chaotic vibration related to system parameters  $x_b$ , this paper selects velocities ( $v = 40.10$  km/h,  $v = 59.30$  km/h and  $v = 64.30$  km/h) in regions A, B and C, respectively [4, 9] to calculate the phase diagram and Poincaré mapping of the system, and focuses on the nonlinear vibration characteristics, which are shown in Fig. 4–6.

The phase diagram in Fig. 4 is a closed curve. At the same time, the Poincaré section is a similarly closed curve. According to the image characteristics of these simulation results, the system makes a quasi-periodic movement within the area of  $40.00$  km/h  $\leq v \leq 50.50$  km/h.

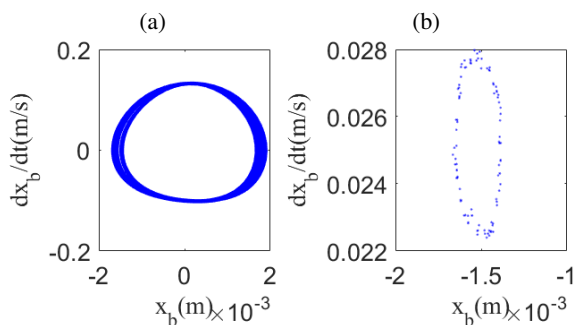


**Fig. 4.** Phase portrait and Poincaré map of  $x_b$  at  $v = 40.10$  km/h

The phase diagram in Fig. 5 consists of multiple closed curves that fill the entire phase space. There are infinitely many points on the Poincaré section. By analyzing the image features, we can conclude that the system is in chaotic movement within the area of  $50.50$  km/h  $\leq v \leq 62.60$  km/h.

We can see from Fig. 6, that there is a great quantity of rings in the form of Hoff rings in the phase diagram. In the Poincaré

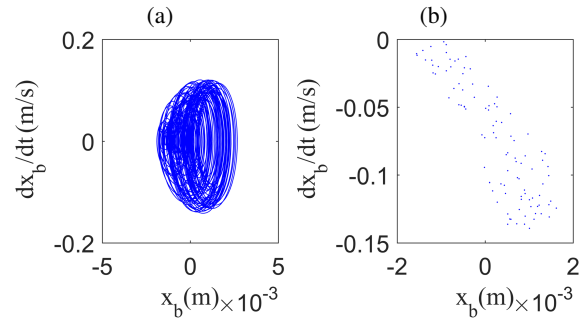


**Fig. 5.** Phase portrait and Poincaré map of  $x_b$  at  $v = 59.30$  km/h

section, a closed ring appears. From the analysis of image features, it can be seen that the system is in the quasi-periodic movement in the range of  $62.60$  km/h  $\leq v \leq 70.00$  km/h.

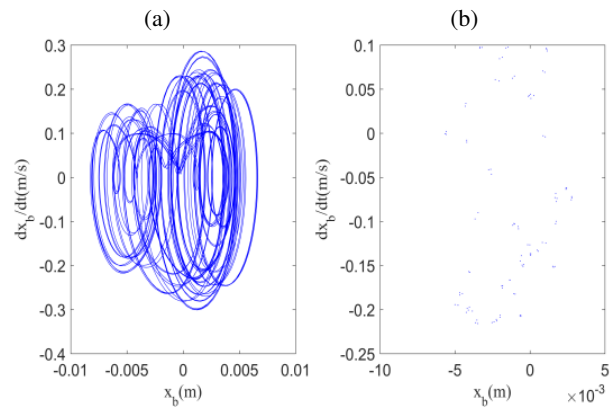


**Fig. 6.** Phase portrait and Poincaré map of  $x_b$  at  $v = 64.30$  km/h

Throughout the above analysis, the vehicle suspension system is stimulated by consecutive SCHs and uneven roads. As the vehicle velocity increases, the nonlinear movement of the system follows a law: quasi-periodic motion  $\rightarrow$  chaotic motion  $\rightarrow$  quasi-periodic motion. The law of motion shows that chaotic movement may happen when the vehicle passes through the combination of trapezoidal and sinusoidal SCHs, and the speed range of chaotic motion is  $50.50$  km/h  $\leq v \leq 60.60$  km/h. Therefore, for passive suspension vehicles, the vehicle speed should not take speed within this range.

## 4. CHAOTIC VIBRATION CONTROL FOR SEMI-ACTIVE SUSPENSION VEHICLES

### 4.1. Design of negative feedback vibration control method

For the sake of suppressing chaotic vibration when the vehicle passes through hybrid SCHs and improving the safety and comfort of passengers, a direct variable feedback control method for a semi-active suspension system is used in this paper. This method achieves chaos control by adding a variable feedback controller to the suspension system and adjusting the value of feedback coefficient  $C$ . This control method for a semi-active suspension system has the advantages of simple design and obvious effect [20, 21].

We can express the  $n$ -dimensional nonlinear chaotic system as:

$$\begin{cases} \dot{x} = F(x(t), t), \\ y = Dx, \end{cases} \quad (9)$$

where  $D$  is a  $1 \times n$  constant matrix,  $F$  is the nonlinear vector function,  $x$  is the system's state which can be represented as  $x = [x_1, x_2, \dots, x_n]^T$ , and  $y$  is the output of the system. We define the variable feedback controller as:

$$U_n = Cx_n \quad n = 1, 2, \dots, n, \quad (10)$$

$C$  is the feedback coefficient, and the feedback controller applied to a nonlinear motion system can be expressed as follows:

$$\dot{x} = F(x(t), t) - U. \quad (11)$$

According to equation (8), the following can be obtained:

$$\begin{cases} \dot{x}_1 = x_2 - U_1, \\ \dot{x}_2 = -\frac{1}{m_b} (F_{sf2} + F_{cf2} + F_{sr2} + F_{cr2}) - g - U_2, \\ \dot{x}_3 = x_3, \\ \dot{x}_4 = \frac{\cos \theta}{J} [(F_{sf2} + F_{cf2}) l_f - (F_{sr2} + F_{cr2}) l_r] - g - U_4, \\ \dot{x}_5 = x_6 - U_5, \\ \dot{x}_6 = -\frac{1}{m_f} (F_{sf2} + F_{cf2} - F_{sf1} + F_{cf1}) - g - U_6, \\ \dot{x}_7 = x_8 - U_7 \\ \dot{x}_8 = -\frac{1}{m_r} (F_{sr2} + F_{cr2} - F_{sr1} + F_{cr1}) - g - U_8. \end{cases} \quad (12)$$

## 4.2. Experiment and analysis

The selection of the appropriate feedback gain coefficient value  $C$  is the key to chaos suppression. Due to the complexity of the nonlinear motion system, theoretical derivation is relatively complicated, so we choose the experimental method to find the appropriate value of  $C$ . To analyze the effect of feedback coefficient on system vibration, we assumed that the speed is 55.00 km/h and  $C$  is in the range of  $0 \leq C \leq 150$ . We drew the bifurcation diagram between the body's vertical displacement  $x_b$  and the feedback coefficient  $C$  through MATLAB simulation, as shown in Fig. 7.

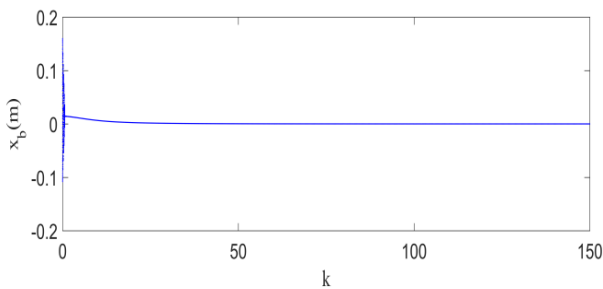


**Fig. 7.** Bifurcation diagrams of the vehicle body's vertical displacement when  $0 < C < 150$

By analyzing the bifurcation diagram from Fig. 7, we can see that with the gradual increasing of the feedback coefficient  $C$  the vertical shift of the car body  $x_b$  decreases gradually towards zero and stabilizes after  $C$  is about 45. To test and verify the influence of direct variable feedback control on the experiment, we took  $C = 50$ , which is greater than 45, as an example, and drew the velocity bifurcation diagram of vertical displacement  $x_b$  under the control of feedback gain coefficient in Fig. 8.

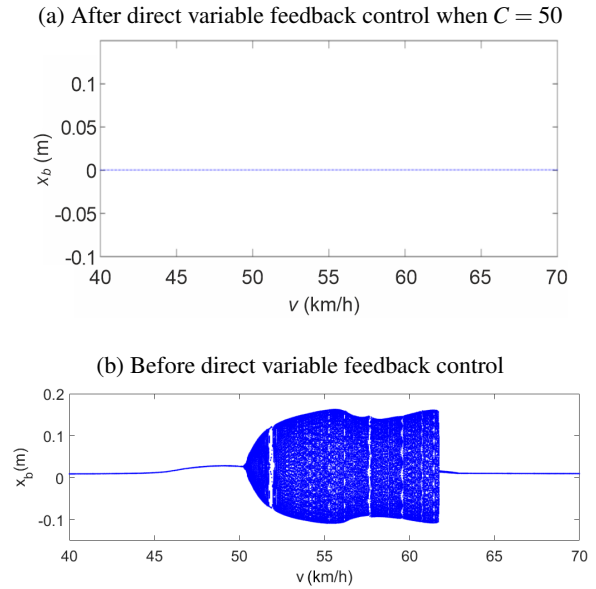


**Fig. 8.** Velocity bifurcation diagram of vertical displacement of the vehicle body

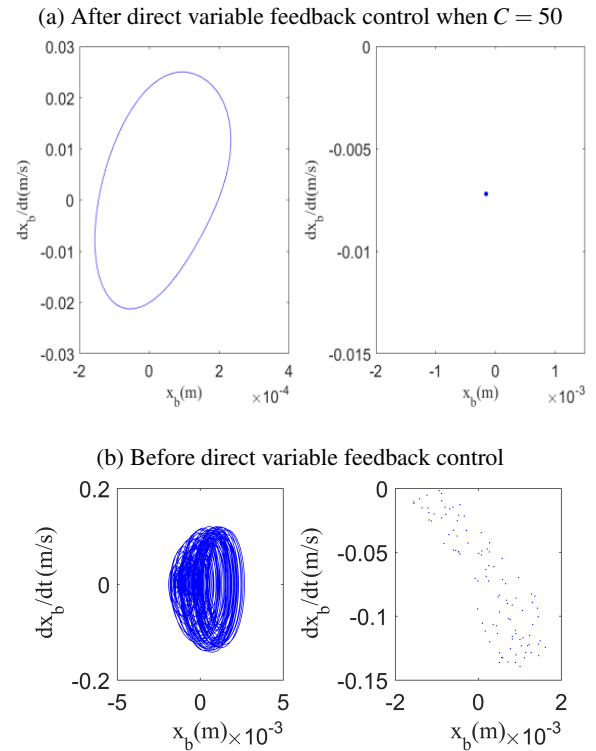


**Fig. 9.** Phase portrait and Poincaré map of  $x_b$  at 59.30 km/h after using variable feedback control

The bifurcation diagram in Fig. 8b is exactly like Fig. 3 that appeared before. By comparing the bifurcation diagram in Fig. 8a with Fig. 8b, it can be seen that the original complex curve of vertical displacement of the car body  $x_b$  has remained almost zero under direct variable feedback control when  $C$  is 50. In order to better verify the effect, we took and plotted the phase diagram and Poincaré map, as shown in Fig. 9.

From Fig. 9a, we can see that the phase diagram presents itself as a closed curve, while the Poincaré map presents itself as a point. Compared with Fig. 9b, which is just like Fig. 5, it can be seen that under the control of direct variable feedback, the system changes from chaotic motion to periodic motion at the speed of  $v = 59.30$  km/h. This proves that the direct variable feedback control method can effectively suppress chaotic vibration.

## 5. MULTI-OBJECTIVE OPTIMIZATION METHOD OF ACTIVE SUSPENSION VEHICLE BASED ON GENETIC ALGORITHM

### 5.1. Multi-objective optimization model design

Active suspension means active control, including equipment that provides energy and additional devices that can control force: active control forces of rear suspensions  $F_{ru}$  and active control forces of front suspensions  $F_{fu}$ , which are shown in Fig. 2 and can meet the requirements of vehicle ride comfort and stability at the same time [22].

In order to measure the comfort of the vehicle, the paper selects displacement  $x_b$  and pitch angle of the vehicle body  $\theta$  as the index [23], combined with equation (8), and establishes the multi-objective functions as follows:

$$f_1 = x_b = x_1, \quad (13)$$

$$f_2 = \theta = x_3. \quad (14)$$

After taking the root-mean-square (RMS) of the two sub-objective functions and de-dimension processing, the linear weighting method is adopted to obtain the total objective function as follows:

$$F = \min \{ \omega_1 \text{RMS}(f_1) + \omega_2 \text{RMS}(f_2) \} \quad (15)$$

$\omega_1$ ,  $\omega_2$  are the weight coefficients of the corresponding term, and we take 0.5 and 0.5 as an example.

For the active suspension vehicle, when passing through the SCHs, vehicle speed  $v$ , active control force of the front suspension  $F_{fu}$  and active control force of the rear suspension  $F_{ru}$  are adjustable parameters that have an impact on the comfort. Therefore, these three parameters are selected as the design variables, and the constraint conditions are:  $0 \text{ km/h} < v \leq 60 \text{ km/h}$ ,  $-2000 \text{ N} < F_{fu} \leq 2000 \text{ N}$ ,  $-2000 \text{ N} < F_{ru} \leq 2000 \text{ N}$ . And before optimization, it is assumed that  $v = 25 \text{ km/h}$ ,  $F_{fu} = 0 \text{ N}$ ,  $F_{ru} = 0 \text{ N}$ .

The multi-objective optimization model mainly uses the idea of GA for reference [24]. Several vehicle comfort indices are selected to establish the multi-objective function, and then the vehicle speed and active control force are taken as design variables to continuously run in cycles in order to generate new populations, select, crossover and mutate. After reaching the maximum evolutionary generation, the optimal chromosome individual is output, that is, the optimized optimal speed and active control force.

The main steps of the optimization model based on GA are shown in Fig. 10. The model takes the reciprocal of objective function  $F$  as the fitness function, sets the population size to 25, and calculates the fitness of each individual in the population. The higher the fitness is, the better the individual is considered. Roulette algorithm is used for the selection operation, so that the larger fitness of individuals indicates the higher probability of entering the next generation of a new population. The crossover operation simulates the mating between individuals, and the crossover rate is set to 0.7. Mutation operation simulates gene mutation, and the mutation rate is set to 0.1. When generating a new population, the elite strategy is used to keep the chromosomes of the best individuals from being destroyed. The maximum evolutionary generation value is set to 250. After the evolution is completed, the parameter values of the optimal individual are obtained.

### 5.2. Experiment and analysis of optimization model

After the experiment with the multi-objective optimization model after 250 generations of genetic evolution,  $v$  of the optimal individual is 50.34 km/h,  $F_{fu}$  is 1143 N and  $F_{ru}$  is 1023 N.

As can be seen from Fig. 11, optimal fitness is roughly taken to the optimal value at around 150 generations, and  $v$  begins to stabilize between 100 and 150 generations,  $F_{fu}$  converges from 100 to 150 generations, and  $F_{ru}$  remains unchanged at about 200 generations. We draw the system response diagram

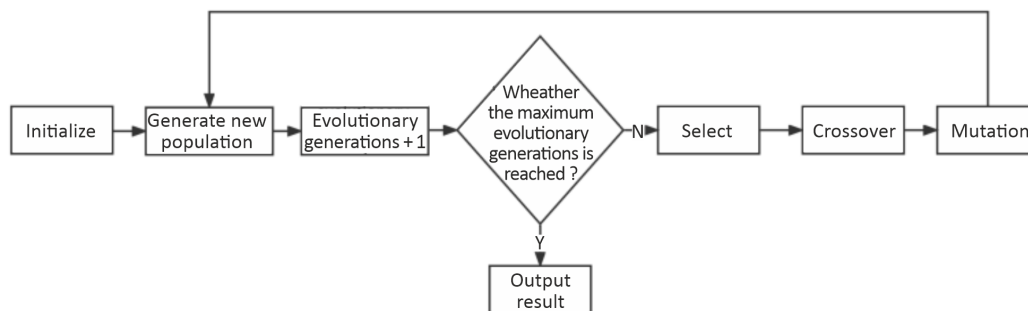


Fig. 10. Steps of multi-objective optimization model based on genetic algorithm

Analysis and control of nonlinear vibration of autonomous vehicle passing through hybrid consecutive speed control humps

of each parameter when the optimized suspension system enters the steady state, and compare it with the response curve of the vehicle before optimization.

Through the analysis of Fig. 12 and Table 3, we can see that the system response values and the RMS of the body verti-

cal displacement, pitch angle and objective function value of the optimized suspension system are significantly lower than those before the optimization, which proves the effectiveness of the optimization model. Meanwhile, performance is improved by 59.02%.

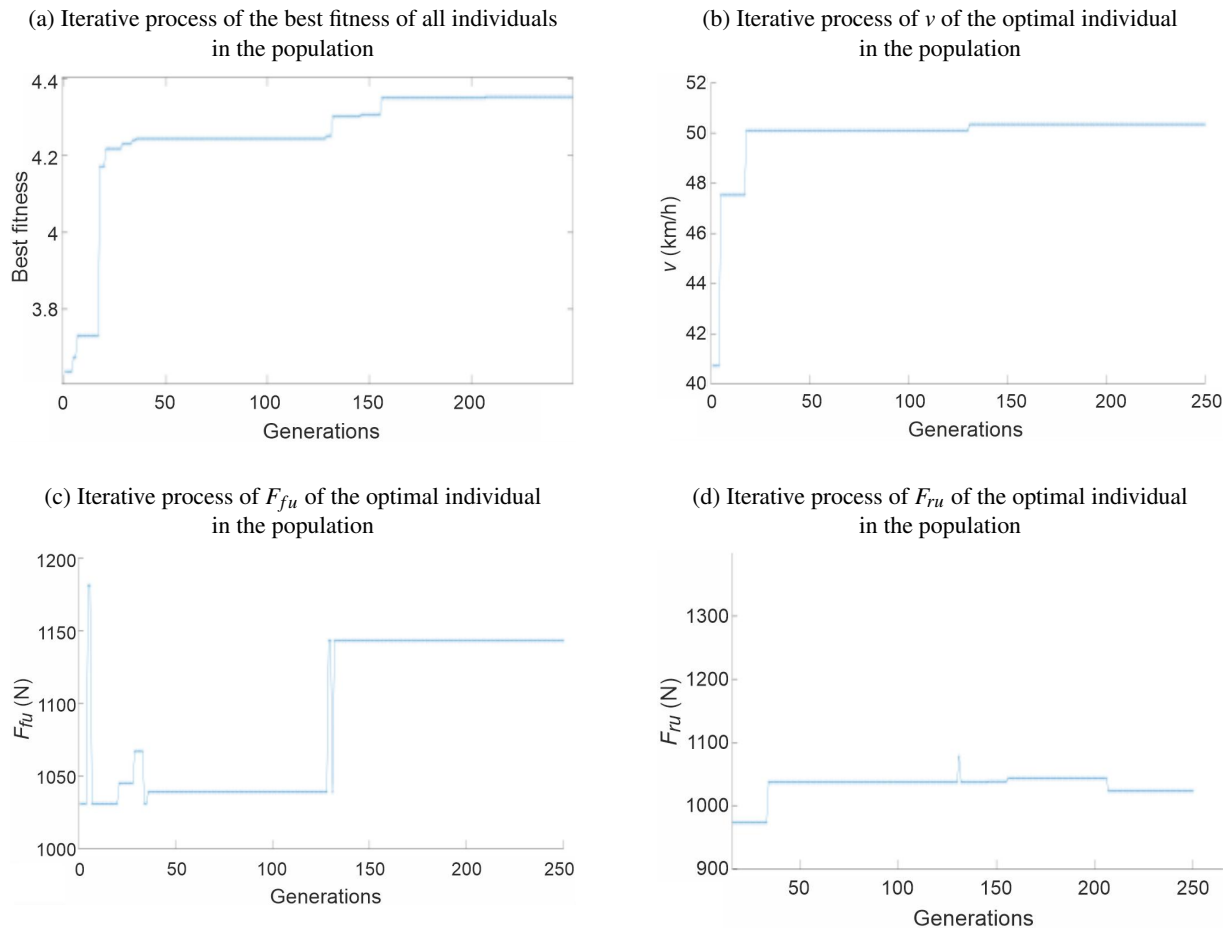


Fig. 11. Iterative processes of each design variable of the optimization model

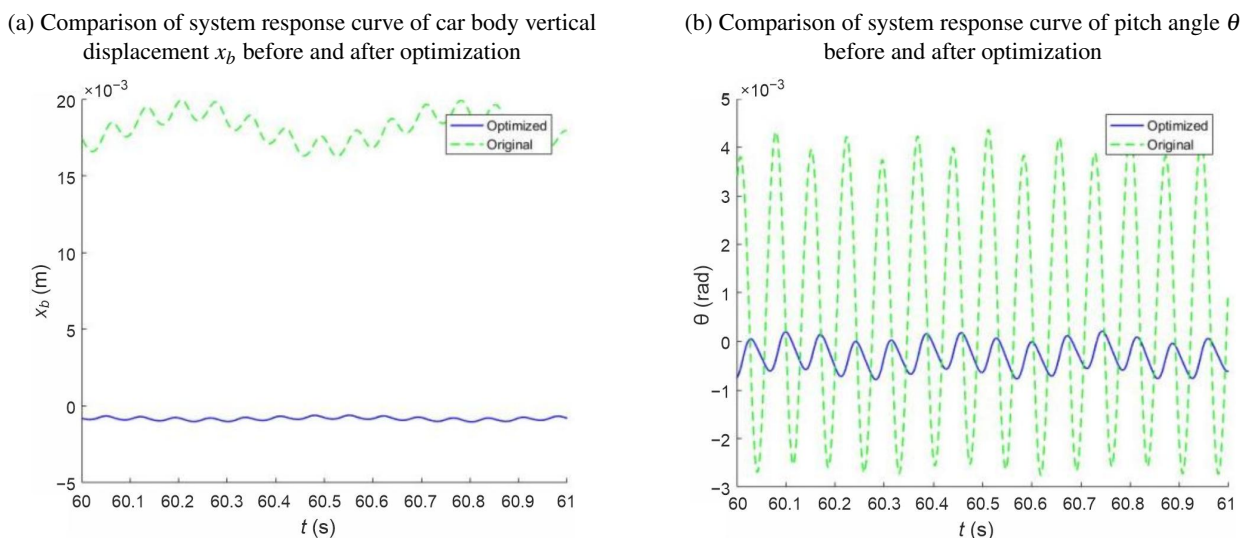


Fig. 12. System response curve of each index after optimization and before optimization

**Table 3**

Comparison of indices and parameters after optimization

State	Before optimization	After optimization
$v$ (km/h)	25	50.34
$F_{fu}$	0	1143
$F_{ru}$	0	1023
The RMS of $x_b$ (m)	0.0225	0.0087
The RMS of $\theta$ (rad)	0.0064	0.0031
The RMS of $F$	0.5774	0.2362
Percentage of overall performance improvement	0	59.02%

## 6. CONCLUSIONS

In this paper, by establishing the SCHs-velocity coupling excitation model and the nonlinear 4-DOF half-vehicle model under the combination of trapezoidal and sinusoidal SCHs, and using bifurcation diagram, phase diagram and Poincaré map obtained by means of simulation experiments, the following conclusions are obtained:

- The nonlinear motion law of vehicles passing this type of hybrid SCHs is as follows: quasi-periodic motion  $\rightarrow$  chaotic motion  $\rightarrow$  quasi-periodic motion.
- For conventional passive suspension vehicles, chaotic vibration may occur when the vehicle passes through hybrid SCHs, and the critical velocity is 50.50 km/h and 62.60 km/h, therefore, it is inappropriate to take the value of this range for speed.
- For semi-active suspension vehicles, we use a direct variable feedback control method and study the influence of feedback gain coefficient on system vibration, and prove the effectiveness of the chaotic vibration control method by comparison.
- For vehicles with active suspension, the optimization model based on GA proposed in this paper can obtain the optimal speed and active control force of the vehicle passing through hybrid SCHs, which effectively improves the comfort of passengers.

The conclusion of this paper can provide the theoretical foundation for speed adaptive control and the research on safety and comfort when the autonomous vehicle passes through hybrid SCHs. It also provides a simple and effective chaotic vibration control idea for the design of the vehicle suspension system. The conclusion and idea can be verified and further improved by follow-up real-vehicle experiments.

## ACKNOWLEDGEMENTS

The authors would like to express gratitude to the anonymous commentators for their valuable suggestions, and to the Fundamental Research Funds for the Program for Innovation Research Groups at Institutions of Higher Education in Chongqing (CXQT21032), and the Fundamental Research Funds for the Natural Science Foundation of Chongqing, China (cstc2021ycjh-bgzxm0088) for support.

## REFERENCES

- [1] C. Wang, X. Zhao, R. Fu, and Z. Li, "Research on the comfort of vehicle passengers considering the vehicle motion state and passenger physiological characteristics: Improving the passenger comfort of autonomous vehicles," *Int. J. Environ. Res. Public Health.*, vol. 17, p. 6821, 2020, doi: [10.3390/ijerph17186821](https://doi.org/10.3390/ijerph17186821).
- [2] Z. Zhenglong, S. Bin, L. Jiangang, D. Zhiguang, and H. Zhongbo, "Research on ride comfort performance of a metal tire," *Bull. Pol. Acad. Sci. Tech. Sci.*, vol. 68, no. 3, pp. 491–502, 2020, doi: [10.24425/bpasts.2020.133384](https://doi.org/10.24425/bpasts.2020.133384).
- [3] L. Zhao, J. Guo, Y. Yu, X. Li, and C. Zhou, "Simulation of nonlinear vibration responses of cab system subject to suspension damper complete failure for trucks," *Int. J. Model. Simul. Sci. Comput.*, vol. 11, no. 2, p. 2050017, 2020, doi: [10.1142/s1793962320500178](https://doi.org/10.1142/s1793962320500178).
- [4] S. Liang, C.G. Li, Q. Zhu, and Q. Y. Xiong, "The influence of parameters of consecutive speed control humps on the chaotic vibration of a 2-DOF nonlinear vehicle model," *J. Vibroeng.*, vol. 13, no. 3, pp. 406–413, 2011.
- [5] Q. Zhu and M. Ishitobi, "Chaos and bifurcation in nonlinear vehicle model," *J. Sound Vib.*, vol. 275, no. 3–5, pp. 1136–1146, 2004, doi: [10.1016/j.jsv.2003.10.016](https://doi.org/10.1016/j.jsv.2003.10.016).
- [6] A. Sezgin and Y. Z. Arslan, "Analysis of the vertical vibration effects on ride comfort of vehicle driver," *J. Vibroeng.*, vol. 14, no. 2, pp. 559–571, 2012, doi: [10.1016/j.jbiomech.2012.01.047](https://doi.org/10.1016/j.jbiomech.2012.01.047).
- [7] G. Litak, M. Borowiec, M. I. Friswell and W. Przystupa, "Chaotic response of a quarter car model forced by a road profile with a stochastic component," *Chaos Solitons Fractals*, vol. 39, no. 5, pp. 2448–2456, 2009, doi: [10.1016/j.chaos.2007.07.021](https://doi.org/10.1016/j.chaos.2007.07.021).
- [8] G. Liu, K. Nonami, and T. Hagiwara, "Semi-active fuzzy sliding mode control of full vehicle and suspensions," *J. Vib. Control*, vol.11, no. 8, pp. 1025–1042, 2008, doi: [10.1177/1077546305053399](https://doi.org/10.1177/1077546305053399).
- [9] S. Liang, Y. S. Sun, and Q. Zhu, "Ride comfort analysis of a nonlinear vehicle excited by the consecutive speed-control humps," *J. Vibroeng.*, vol. 15, no. 4, pp. 1656–1664, 2013.
- [10] Z.Y. Yang, S. Liang and Q. Zhu, "Chaotic vibration and comfort analysis of nonlinear full-vehicle model excited by consecutive speed control humps," *Math. Probl. Eng.*, vol. 2014, pp. 1–8, 2014, doi: [10.1155/2014/370634](https://doi.org/10.1155/2014/370634).
- [11] H. Gheibollahi and M. Masih-Tehrani, "Optimal speed control humps design based on driver comfort," *Int. J. Automot. Mech. Eng.*, vol. 18, no. 3, pp. 8941–8958, 2021, doi: [10.15282/ijame.18.3.2021.08.0685](https://doi.org/10.15282/ijame.18.3.2021.08.0685).
- [12] J. Fakhraei, H.M. Khanlo, M. Ghayour, and K. Faramarzi, "The influence of road bumps characteristics on the chaotic vibration of a nonlinear full-vehicle model with driver," *Int. J. Bifurcation Chaos*, vol. 26, no. 9, p. 1650151, 2016, doi: [10.1142/S0218127416501510](https://doi.org/10.1142/S0218127416501510).
- [13] Z.Y. Yang, S. Liang and Y.S. Sun, "Vibration suppression of four degree-of-freedom nonlinear vehicle suspension model excited by the consecutive speed humps," *J. Vib. Control*, vol. 22, no. 6, pp. 1560–1567, 2014, doi: [10.1177/1077546314543728](https://doi.org/10.1177/1077546314543728).
- [14] M. Deng, Z. Wu, Z. Yao and Y. Chen, "Unmanned aerial vehicle jamming resource scheduling based on parallel genetic algorithm with elite set," *J. Electron. Inf. Technol.*, vol. 44, pp. 2158–2165, 2022, doi: [10.11999/JEIT210349](https://doi.org/10.11999/JEIT210349).
- [15] W. Wang, M. Niu and Y. L. Song, "Integrated vibration control of in-wheel motor-suspensions coupling system via dynamics parameter optimization," *Shock Vib.*, vol. 2019, p. 3702919, 2019, doi: [10.1155/2019/3702919](https://doi.org/10.1155/2019/3702919).

- [16] P. Guo and J.H. Zhang, "Numerical model and multi-objective optimization analysis of vehicle vibration," *J. ZheJiang Univ.-Sci. A*, vol. 18, no. 5, pp. 393–412, 2017, doi: [10.1631/jzusA1600124](https://doi.org/10.1631/jzusA1600124).
- [17] W. Sun, Y. Li, J. Huang, and N. Zhang, "Efficiency improvement of vehicle active suspension based on multi-objective integrated optimization," *J. Vib. Control*, vol. 23, pp. 539–554, 2017, doi: [10.1177/1077546315581731](https://doi.org/10.1177/1077546315581731).
- [18] R.R.M.R. da Silva, I.L. Reinaldo, D.P. Montenegro, G.S. Rodrigues, and E.D.R. Lopes, "Optimization of vehicle suspension parameters based on ride comfort and stability requirements," *Proc. Inst. Mech. Eng., Part D: J. Automob. Eng.*, vol. 235, pp. 1920–1929, 2021, doi: [10.1177/0954407020983057](https://doi.org/10.1177/0954407020983057).
- [19] Z.Y. Yang, L. Wang, F.T. Liu, and Z.J. Li, "Nonlinear dynamic analysis of constant-speed and variable-speed of autonomous vehicle passing uneven road," *J. Vibroeng.*, vol. 24, no. 4, pp. 726–744, 2022, doi: [10.21595/jve.2022.22250](https://doi.org/10.21595/jve.2022.22250).
- [20] Z.Y. Yang, S. Liang, Y. Sun, and Qin Zhu, "Chaotic vibration and control in nonlinear half-vehicle suspension under consecutive humps excitation," *2014 International Conference on Advanced Mechatronic Systems*, 2014.
- [21] Z.Y. Yang, S. Liang, Y.S. Sun, and Q. Zhu, "Vibration suppression of four degree-of-freedom nonlinear vehicle suspension model excited by the consecutive speed humps," *J. Vib. Control*, vol. 22, no. 6, pp. 1560–1567, 2016, doi: [10.1177/1077546314543728](https://doi.org/10.1177/1077546314543728).
- [22] G.W. Lee, M. Hyun, D.O. Kang, and S.J. Heo, "High-efficiency active suspension based on continuous damping control," *Int. J. Automot. Technol.*, vol. 23, no. 1, pp. 31–40, 2022, doi: [10.1007/s12239-022-0003-4](https://doi.org/10.1007/s12239-022-0003-4).
- [23] G. Tran, T. Pham, O. Sename, E. Costa, and P. Gaspar, "Integrated comfort-adaptive cruise and semi-active suspension control for an autonomous vehicle: An LPV approach," *Electronics*, vol. 10, no. 7, pp. 813, 2021, doi: [10.3390/electronics10070813](https://doi.org/10.3390/electronics10070813).
- [24] L. Wang, Z.Y. Yang, X.D. Chen, R.X. Zhang, and Z. Yu, "Research on adaptive speed control method of an autonomous vehicle passing a speed bump on the highway based on a genetic algorithm," *Int. J. Mech. Sci.*, vol. 13, no. 2, pp. 647–657, 2022, doi: [10.5194/ms-13-647-2022](https://doi.org/10.5194/ms-13-647-2022).